Sustainable Food Technology

ROYAL SOCIETY OF CHEMISTRY

PAPER

View Article Online
View Journal | View Issue

Cite this: *Sustainable Food Technol.*, 2026, **4**, 772

Multi-pin cold plasma treatment of chia (*Salvia hispanica* L.) seeds: nutritional & anti-nutritional, techno-functional, and structural properties

Aashita Bhardwaj, [a] Chetna Singh, [a] Rachna Sehrawat, [b] Vijay Singh Sharanagat [c] and Tanya Luva Swer *[a]

The present study focused on multi-pin cold plasma treatment (CPT, voltage- 10, 20, and 30 kV, time- 10, 20, and 30 min) to investigate the nutritional, antinutritional, techno-functional, and structural properties of chia seed flour (*Salvia hispanica* L.). CPT significantly ($p \leq 0.05$) enhanced the protein content (22.84 to 24.63%), water absorption capacity (9.17 to 12.16 g g^{-1}), oil absorption capacity (0.74 to 1.53 g g^{-1}), swelling power (9.17 to 12.16 g g^{-1}), *in vitro* protein digestibility (65.92 to 72.68%) and improved pasting and thermal stability of chia seed flour. It reduced the amount of anti-nutritional compounds, *i.e.*, tannins (3.48 to 2.88 mg TAE per g) and phytates (2.15 to 1.53 mg PAE per g), resulting in improved *in vitro* digestibility and mineral content. FTIR spectra suggested potential modification of functional groups, while XRD analysis indicated reduced crystallinity with increasing voltage and time. The SEM images revealed surface disruption with increased porosity in plasma-treated samples. Principal component analysis displayed a favourable correlation between moderate plasma exposure (20 kV) and durations (10–20 min) with enhanced chia seed flour properties. CPT proves to be an effective non-thermal technology for improving the nutritional and techno-functional properties of chia seed flour, which could potentially enhance its diverse applications in food and nutraceutical formulations.

Received 10th September 2025
Accepted 29th October 2025

DOI: 10.1039/d5fb00582e

rsc.li/susfoodtech

Sustainability spotlight

The application of multi-pin cold plasma to chia seeds (*Salvia hispanica* L.) demonstrates a resource-efficient, chemical-free processing approach that preserves nutritional quality while modulating anti-nutritional components and improving the techno-functional and structural characteristics of the flour. Operating at atmospheric pressure and near-ambient temperatures, this technique minimizes energy and water use, reduces chemical inputs, and aligns with sustainable food processing and circular economy principles, offering an environmentally responsible strategy for value-added chia-based ingredients.

1 Introduction

Chia seeds, derived from the perennial herb *Salvia hispanica* L. of the family Labiatae or Lamiaceae, are often categorized as oilseeds as well as pseudocereals.[1] It has been mainly cultivated in Mexico, Guatemala, and the western parts of Central and Southern America since early 3500 BCE.[2] The crop is resilient to arid and semi-arid regions, making it one of the important components of the diet of the Mesoamericans in the Aztec and Mayan civilizations.[3] It also holds cultural and economic significance, often being used as offerings in rituals or even as currency in trade until the onset of colonialism.[4] The 20th century witnessed the resurgence of chia seeds owing to tremendous research work demonstrating their health-benefiting properties, thus attracting health-conscious consumers. With this growing awareness and the extensive scientific observations, chia seeds were reintroduced as a superfood, resulting in widespread cultivation, with Mexico, Argentina, and Australia becoming the main producers.[5] This revival is not only attributed to its historical significance but also backed by scientific validation, whereby by the year 2000, chia seeds became established in health food stores and supermarkets worldwide as they were increasingly incorporated in numerous food items.[6] According to US dietary regulations, chia seeds can be eaten raw or as sprouts and added to salads, drinks, and cereal dishes.[7] Chia seeds are nutritionally dense, having a higher amount of protein (19–23 g/100 g), fat (30–33 g/100 g), carbohydrates (40 g/100 g), and dietary fiber (34–40 g/100 g) and being rich in α-linolenic and crucial omega-3 fatty acid.[8] They have a higher amount of calcium, potassium, and

[a]*Department of Food Science and Technology, National Institute of Food Technology Entrepreneurship and Management, Kundli, Haryana 131028, India. E-mail: aashi1912@gmail.com; chetnasingh455@gmail.com; tanyaswer@gmail.com*

[b]*Department of Food Process Engineering, National Institute of Technology, Rourkela, Odisha 769008, India. E-mail: sehrawatr@nitrkl.ac.in*

[c]*Department of Food Engineering, National Institute of Food Technology Entrepreneurship and Management, Kundli, Haryana 131028, India. E-mail: vijaysinghs42@gmail.com*

magnesium compared to milk. The rich nutritional profile of chia seeds is linked to several health benefits, such as a lower risk of obesity, inflammation, type II diabetes, and heart disease.[4,9] Additionally, its gluten-free nature makes it a superfood and suitable for people suffering from celiac disease or gluten intolerance.[10] Despite its rich nutritional profile, the application of chia seed flour is limited due to its poor functional characteristics and poor physical properties of developed food products.[11] Hence, researchers have explored different processing techniques (roasting, cooking, and germination) to enhance the functional properties of chia seed flour.[12–15] However, these processes have certain limitations, such as long processing time and degradation of heat-sensitive compounds (beneficial fatty acids and antioxidants),[16] formation of harmful heat-induced compounds like acrylamide[17] and a reduction in water-holding capacity.[18] Hence, there is a need for a short-time and moderate temperature process to prevent and enhance the nutritional benefit and functional characteristics for versatile application of chia seed flour in food and pharma.

Among various novel non-thermal technologies, cold plasma stands out as a versatile processing method. Cold plasma is composed of reactive species like electrons, free radicals, excited gas atoms, ions, and molecules.[19] These reactive species initiate numerous chemical reactions in the target material, such as oxidation, sulfoxidation, nitration, and sulfonation, that lead to surface etching, crosslinking, and depolymerization of food macromolecules like protein, carbohydrates, and lipids.[20] These modifications enhance the functional properties of the food macromolecules, resulting in improved quality and stability of derived food products.[21] Researchers have explored cold plasma treatment (CPT) for various food grains and flour and reported improved nutritional, techno-functional, bioactive, pasting, and morphological properties.[22–30] Although CPT has shown promising improvements in the functionality of various flours, its application to pseudocereals remains relatively unexplored. With the rising demand for gluten-free products and a shift towards non-thermal processing methods over conventional techniques, chia seeds are less explored, and researchers have mainly focused on atmospheric pressure cold plasma (ACP) induced technological characteristics, phenolic and antioxidant activities,[31] nutritional characteristics,[32] modification of chia seed mucilage,[33] physicochemical properties of soy protein isolate-chia seed gum complex,[34] and mucilage extraction.[35]

Considering the limited work on cold plasma-induced modification of chia seeds for their application in food formulations, the present study is focused on multipin cold plasma discharge treatment on physicochemical, nutritional, anti-nutritional, techno-functional, pasting behaviour, and molecular interactions of chia seed flour under varying voltages and exposure time. Multipin cold plasma discharge generates plasma with multiple fine-point pin emitters, covering a wider surface area compared to conventional single-pin systems. Moreover, it consumes less power and operates at relatively lower plasma voltages than DBD, ensuring a uniform discharge across the surface of the food product.[27,36]

2 Materials and methods

2.1 Raw materials and chemicals

Chia seeds were procured online from True Elements Company (Maharashtra, India). The seeds were properly cleaned, and any foreign matter was removed. Later, the seeds were stored in an airtight plastic bag and kept at room temperature (28 ± 2 °C) until treatment was applied. The chemicals used in the study, including ammonium ferric sulphate, ammonium chloride, bipyridine, hydrochloric acid, nitric acid, ethanol, phytic acid, sodium hydroxide, sodium salt hydrate, sodium carbonate, sulfuric acid, tannic acid, thioglycolic acid, and vanillin, were purchased from SRL Pvt Ltd (India). Standards including α-chymotrypsin, 2,2-diphenyl-1-picrylhydrazyl (DPPH), Folin–Ciocalteu reagent (FC), gallic acid (GA), peptidase, quercetin, and trypsin were purchased from Himedia, India. All the other chemicals and reagents used for the present study were of analytical grade.

2.2 Cold plasma treatment

Chia seeds were treated with a multipin plasma discharge system (IN-HVLT MP, Ingenium Naturae Private Limited, Gujarat, India) having an input voltage of 230 V and frequency of 50 Hz from the main supply and a maximum output voltage of 60 kV (Fig. 1). It has two stainless steel electrodes 3 cm apart, containing 63 high voltage pins with a total discharge area of 185 × 250 mm, and it uses ambient air for plasma generation.[27] For treatment, 50 g of whole chia seeds were spread evenly (1 to 2 mm thickness) on a Petri plate and exposed to output voltages of 10, 20, and 30 kV for 10-, 20-, and 30-minutes durations, respectively. After the treatment, chia seed samples were milled using a grinder (Hamilton Beach, 58770-IN) and passed through a 600 μm mesh sieve and stored in airtight zipper bags at −18 °C until further analysis. The treated samples were coded as follows: T1 (10 kV – 10 min), T2 (10 kV – 20 min), T3 (10 kV – 30 min), T4 (20 kV – 10 min), T5 (20 kV – 20 min), T6 (20 kV – 30 min), T7 (30 kV – 10 min), T8 (30 kV – 20 min), T9 (30 kV – 30 min). Untreated chia seed flour was taken as the control.

2.3 Physicochemical properties

2.3.1 Bulk density (BD) and tapped density (TD). Bulk density (BD) and tapped density (TD) of the flour samples were determined by the methods of Joy *et al.* (2022).[26] A sample of 20 g was transferred to a 50 mL measuring cylinder, and the initial volume was noted to calculate the BD. The cylinder was tapped 100 times on a rubber bottom. The final volume obtained after tapping was measured to determine the TD. BD and TD were calculated using the following formulae:

$$\mathrm{BD}\left(\mathrm{g\ mL^{-1}}\right) = \frac{W_s}{V_s} \quad (1)$$

$$\mathrm{TD}\left(\mathrm{g\ mL^{-1}}\right) = \frac{W_s}{V_t} \quad (2)$$

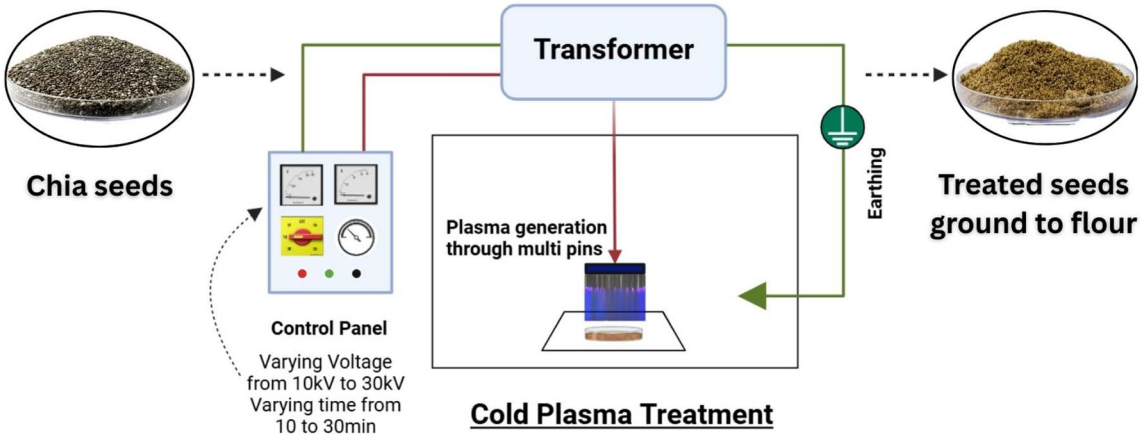

Fig. 1 Schematic representation of the cold plasma treatment setup.

where,

W_s – sample weight, V_s – volume of sample before tapping, V_t – volume of sample after tapping.

2.3.2 Colour. The colour values (L^*, a^*, b^*) of all samples were assessed using a chromameter (CR-400 Konica Minolta Optics, Japan).[30] The total colour difference (ΔE) was calculated using the following expression:

$$\Delta E = \sqrt{(\Delta L^*)^2 + (\Delta a^*)^2 + (\Delta b^*)^2} \quad (3)$$

where ΔL^*, Δa^*, and Δb^* are the differences in lightness, red/green, and yellow/blue, respectively, between the respective treated and control samples.

2.4 Functional and gel hydration properties

2.4.1 Water absorption capacity (WAC) and oil absorption capacity (OAC). The water and oil absorption capacities of the chia seed flour samples were determined following the methods outlined by Hatamian *et al.* (2020) with slight modifications.[13] The sample was suspended in distilled water (DW) (1 : 20, w v^{-1}). The suspension was vortexed and allowed to stand for 30 min to ensure proper hydration. This suspension was centrifuged at 3000×*g* for 15 min (Sigma 3-18KS) and the supernatant was decanted. The tubes were inverted to remove any residual fluid. The weight of the drained residue was noted. The following formula was used to calculate the WAC and OAC of samples.

$$\text{WAC or OAC}(\text{g g}^{-1}) = \frac{W_r}{W_s} \quad (4)$$

where W_r is the residue weight and W_s is the sample weight.

2.4.2 Emulsifying capacity (EC) and emulsifying stability (ES). The emulsifying properties of the flour samples were determined using the method of Chandra *et al.* (2014) with minor changes.[37] The sample (1 g) was added to 15 mL of DW and 7 mL of sunflower oil, and the mixture was first vortexed and then homogenized at 10 000 rpm for 3 min using a homogenizer (Igene Labserve IG-HT-500) to obtain an emulsion. This was followed by centrifugation at 2000×*g* for 30 min. The emulsion volume was measured and noted. For emulsion stability, the emulsion was subject to heating at 80 °C for 30 min. The heated emulsion was cooled to room temperature (28 ± 2 °C) and then centrifuged at 1200×*g* for 15 min. EC and ES were calculated using the following formula:

$$\text{EC or ES}(\%) = \frac{H_l}{H_w} \times 100 \quad (5)$$

where H_l is the height of the emulsified layer and H_w is the height of the whole layer.

2.4.3 Gel hydration properties. The water absorption index (WAI), water solubility index (WSI), and swelling power (SP) of the flour samples were analyzed according to the procedures of Chaple *et al.* (2020).[24] The sample was dispersed in DW (1 : 20, w v^{-1}). The dispersion was heated to 90 °C for 10 min, cooled, and then centrifuged at 3000×*g* for 10 min. The supernatant was collected and dried in a hot air oven at 105 °C until a constant weight was obtained. The weights of the residue after centrifugation (W_r) and the dry solids of the supernatants after drying (W_s) were noted. The WAI, WSI, and SP were calculated using the formulae below.

$$\text{WAI (g g}^{-1}) = W_r/W_i \quad (6)$$

$$\text{WSI (g g}^{-1}) = W_s/W_i \quad (7)$$

$$\text{SP (g g}^{-1}) = W_r/(W_i - W_s) \quad (8)$$

2.5 Nutritional evaluation

2.5.1 Proximate composition. The proximate composition of the control and treated flour samples was estimated according to the official AOAC (2000) methods, using advanced high-precision equipment. All measurements were performed under controlled laboratory conditions in triplicate. Protein content was estimated using the Kjeldahl system (KDI050, Labquest), fat content using a Soxotherm (Gerhardt), and fiber content using an FES06 RTS (Fibraplus). The total carbohydrate content was determined by the difference method by

subtracting the sum of moisture, fat, protein, and ash from 100. The energy value was determined using the Atwater factors.[38]

2.5.2 Mineral profile. The mineral profile of chia seed flour, including the contents of calcium (Ca), magnesium (Mg), potassium (K), phosphorus (P), iron (Fe), zinc (Zn), copper (Cu), and manganese (Mn), was determined following the wet digestion method using HNO_3 and H_2O_2. Quantification was performed using an Inductively Coupled Plasma Optical Emission Spectrophotometer (PerkinElmer, Optima 7000 DV-ICP/OES, USA).[39]

2.5.3 *In vitro* protein digestibility (IVPD). The *in vitro* protein digestibility (IVPD) of the flour samples was determined using a multienzyme mixture (trypsin, α-chymotrypsin, and peptidase), and the final pH was measured for each sample post incubation (37 °C for 10 min).[40] The following formula was used to determine the digestibility of all samples.

$$\mathrm{IVPD} = 210.46 - 18.103z \quad (9)$$

where z is the final pH.

2.5.4 Antioxidant properties. Total phenolic content (TPC), total flavonoid content (TFC), and antioxidant activity (AOA) were determined following the methods described by Kheto *et al.* (2022).[41] Each sample was dispersed in 80% ethanolic solution in the ratio of 1 : 25 (w v^{-1}) in a covered conical flask. The flask was placed in a shaker incubator (New Brunswick, Innova 42R Inc/Ref shaker) at 25 °C and orbital speed of 100 rpm. After 24 h of extraction, the dispersion was subjected to centrifugation at 3000×*g* for 10 min at 4 °C. The supernatant obtained was filtered to obtain a clear extract and stored at 4 °C until being analyzed. To determine the TPC, a 0.1 mL aliquot of the extract obtained was mixed with 2.5 mL of 10% FC reagent and 2.0 mL of 7.5% Na_2CO_3. The mixture was incubated at 45 °C for 40 min. The absorbance was measured at 765 nm using a UV spectrophotometer (Multiskan Skyhigh 1550, Singapore). TPC was expressed as mg gallic acid equivalent per 100 gram (mg GAE/100 g). Additionally, the TFC of all samples was analyzed by briefly taking 0.5 mL of the extract and mixing sequentially with 0.5 mL of methanol, 4 mL of DW, and 0.3 mL of 5% $NaNO_2$. The mixture was allowed to stand for 5 min. Then, 0.3 mL of 10% $AlCl_3$ was added and allowed to equilibrate for 6 min. After 6 min, 2 mL of 1 M NaOH and 2.4 mL of DW were added and mixed. The mixture was kept at room temperature (28 ± 2 °C) for 15 min, and then the absorbance was recorded at 510 nm. The results were expressed as mg quercetin equivalent per gram (mg QE per g). Further, the antioxidant activity (AOA) of the samples was measured by the DPPH assay. An aliquot of 2 mL of extract was mixed with 3.9 mL of DPPH solution (0.2 mM in ethanol) and the mixture incubated for 30 min. The absorbance was taken at 517 nm, and the AOA of the samples was calculated using the following equation:

$$\mathrm{AOA}(\%) = \frac{(\text{Absorbance of control} - \text{Absorbance of sample})}{\text{Absorbance of control}} \times 100 \quad (10)$$

2.5.5 Anti-nutritional factors. The total tannin and phytic acid contents were determined according to the methods given by Patra *et al.* (2024).[30] To analyse the total tannin content (TTC), approximately 0.2 g of sample was extracted in 5 mL of 1% acidified methanol for 15 h at room temperature (28 ± 2 °C). The mixture was centrifuged at 8000 rpm for 15 min. The supernatant obtained was mixed with 5 mL of vanillin–HCl reagent and incubated for 20 min at room temperature. Absorbance was measured at 500 nm, and TTC was expressed as mg tannic acid equivalent per gram (mg TAE per g). For determining the phytic acid content in samples, 0.5 g of the sample was extracted with 10 mL of 0.2 M HCl. Extraction was conducted in a shaker water bath for 1 h at room temperature and then subjected to centrifugation at 5000 rpm for 15 min. Briefly, 0.5 mL of the supernatant collected was mixed with 1 mL of ammonium ferric sulphate and heated in boiling water for 30 min. The mixture was allowed to cool, and 2 mL of bipyridine solution was added and allowed to stand for 5 min. The absorbance was recorded at 519 nm, and results were expressed as mg phytic acid equivalent per gram (mg PAE per g).

2.6 Pasting properties

The pasting profile of samples was measured according to García-Salcedo *et al.* (2018) using a rheometer (Anton Paar, MCR 52, Austria).[42] The sample was mixed with DW (1 : 12, w v^{-1}) and heated from 50 to 95 °C. This was followed by cooling to 50 °C at a rate of 6 °C min^{-1}. The peak viscosity (PV), breakdown viscosity (BV), final viscosity (FV), setback viscosity (SV), pasting temperature (PT), and peak time (Pt) were recorded for each sample.

2.7 Thermal properties

Thermal properties of the samples were analysed using a Differential Scanning Colorimeter (DSC 200, NETZSCH, Germany). In brief, 4 mg of samples were taken and hermetically sealed in an aluminium crucible and heated from 30 °C to 150 °C at a heating rate of 10 °C min^{-1}. The onset temperature (T_o), peak temperature (T_p), and conclusion temperature (T_c) were recorded for all flour samples.[31]

2.8 Structural and molecular characterization

2.8.1 FTIR spectroscopy. Fourier transform infrared spectroscopy (FTIR) was done to analyze the effect of CPT on the functional groups of the chia seed flour. FTIR spectra were obtained using an FTIR spectrophotometer (ALPHA-II Bruker) in the range 4000 cm^{-1} and 400 cm^{-1} to identify functional groups in the flour samples.[13]

2.8.2 X-ray diffraction (XRD). The crystallinity patterns and structure of the flour samples were obtained using an X-ray diffractometer (Smart Lab, Rigaku Co., Japan) with a scanning range of 5° to 60° (2θ) at 40 mA and 45 kV.[42]

2.8.3 Scanning electron microscopy (SEM). The micrographs for control and CPT flour samples were obtained to visualize their surface morphology using FESEM (JSM-7610F

Plus, JEOL) at 5000x magnification and 2 kV accelerating voltage.[40]

2.9 Statistical analysis

All measurements were carried out in triplicate, and the results were presented as mean ± standard deviation. All the parameters were analyzed by one-way analysis of variance (ANOVA) and Duncan's post hoc test ($p \leq 0.05$) using IBM SPSS software (version 20.0). Principal component analysis (PCA) was used to study the effect of varied treatment conditions on different properties of chia seed flour using Origin Pro software (2018).

3 Results and discussion

3.1 Effect of CPT on the physico-chemical properties of chia seed flour

Bulk density (BD) and tapped density (TD) are essential characteristics of flour in determining its flow, handling, processing, and end-use qualities. Cold plasma incurs a reduction in the moisture of treated flour samples that affects their density.[26] As shown in Table 1, CPT had a significant ($p \leq 0.05$) effect on the BD and TD of chia seed flour ($p \leq 0.05$). This change may be due to the microstructural modifications and surface changes from the etching effect of CPT, which affects the particle size, structure, and molecular arrangement of the flour. These changes improve particle cohesion, resulting in a denser packing structure.[43] The L^* values increased significantly after plasma treatment. Upadhyay *et al.* (2020) reported similar findings, noting that plasma treatment also increased lightness in flour due to the breakdown of polyphenols, which produced a bleaching effect.[44] The a^* and b^* values were found to significantly ($p \leq 0.05$) decrease with higher voltage and treatment time. Total colour change (ΔE) was also significantly different from CPT. Increased voltage and exposure time (T5 to T9) gave a ΔE value exceeding 3, which is normally perceptible to the human eye, showing considerable colour differences likely to impact perception by the human eye and consumer acceptance of the flour. Higher power results in more collisions between gas molecules and electrons in the air, generating greater quantities of oxidizing species, whereas longer treatment exposure allows for increased contact time between oxidizing species and flour, thus resulting in significant colour changes.[45]

3.2 Effect of CPT on the functional properties of chia seed flour

3.2.1 Functional properties. The functional properties of chia seed flour samples were significantly influenced by treatment conditions. From Table 1, it was observed that CPT had a significant ($p \leq 0.05$) effect on the water absorption capacity (WAC) of treated chia seed flour. The WAC of the control sample was 9.17 g g^{-1}. As the treatment conditions were increased, a significant increase in WHC was observed, with the highest value of 12.16 g g^{-1} in T5 (20 kV – 20 min). The plasma treatment induces the formation of microchannels and surface etching on the flour particles, which enhances water penetration through capillary action. Moreover, the reactive oxygen and nitrogen species (RONS) generated during plasma exposure cleave the glycosidic and polymeric bonds, exposing polar hydroxyl groups of mucilage and dietary fiber. Additionally, the interaction of RONS results in the partial unfolding of amino acid side chains, such as –OH, $–NH_2$, and –COOH, thereby exposing additional hydrophilic sites and enhancing the WAC of the treated samples.[22,46] On the other hand, a gradual decrease in WAC was observed at higher voltage levels (30 kV) with increasing treatment time, which can be attributed to the weakening of hydrogen bonds upon prolonged plasma exposure, resulting in a decrease in the accessibility of hydrophilic –OH groups for water binding.[31] This observation is supported by the FTIR spectra in the O–H stretching region (around 3000–3400 cm^{-1}), where higher transmittance was observed. Furthermore, at prolonged treatment durations, the RONS generated by plasma can promote oxidative cross-linking and aggregation of chia proteins. The formation of covalent bonds, such as disulfide and carbonyl linkages, among protein molecules leads to a more compact and rigid network structure, which reduces the exposure of polar sites capable of forming hydrogen bonds with water molecules.[46] These structural alterations result in increased surface hydrophobicity and reduced WAC at longer exposure durations. Similar observations were reported for cold plasma-treated whole wheat flour,[24] jackfruit seed flour[26] and quinoa flour.[47] A high WAC observed for moderate plasma exposure can be especially useful in food products where bulking and a consistent texture are important, such as baked goods.[48] A similar trend was observed for the oil absorption capacity (OAC) of the treated flour samples. The OAC significantly ($p \leq 0.05$) increased with increasing voltage level and exposure time, reaching a peak value of 1.53 g g^{-1} in sample T5 (20 kV – 20 min), which then decreased gradually when further exposed to CPT. The enhanced OAC value at moderate voltage and exposure time may be attributed to the surface alterations caused by plasma treatment. CPT causes the denaturation and decomposition of proteins, disrupting their secondary structure and exposing the hydrophobic groups in the proteins, which increases the affinity of the treated flour to oil.[24] High OAC observed for moderate plasma exposure is suitable for products where oil retention enhances flavour, mouthfeel, and texture, particularly in meat and bakery products.[37] On a similar note, increasing emulsifying capacity (EC) and stability (ES) were also observed in CPT samples in comparison to the control sample. This may be attributed to the higher exposure of hydrophobic amino acid chains in CPT samples, which significantly improves their emulsion properties.[20] These findings also revealed that the treated chia seed flour formed more stable emulsions compared to the control (21.82%), with the maximum value (26.10%) observed for treatments T4 and T5. Kheto *et al.* (2023) also observed a significant increase in the emulsifying capacity and stability of guar seed flour.[40]

3.2.2 Gel hydration properties. The gel hydration properties significantly varied with CPT (Table 1) and the trend was consistent with that of WAC. The water absorption index (WAI) of the control sample was 8.33 g g^{-1} which initially increased significantly ($p \leq 0.05$) upon exposure to plasma at voltages of 10 kV and 20 kV up to a maximum value of 12.66 g g^{-1} in T5 (20

Table 1 Effect of CPT on the physicochemical and functional properties of chia seed flour[a]

Parameters		Control	T1	T2	T3	T4	T5	T6	T7	T8	T9
Physicochemical properties	BD (g ml^{-1})	0.36 ± 0.01^{c}	0.38 ± 0.03^{b}	0.42 ± 0.03^{a}	0.38 ± 0.02^{b}	0.36 ± 0.02^{b}	0.36 ± 0.01^{c}	0.36 ± 0.04^{c}	0.36 ± 0.02^{c}	0.38 ± 0.01^{b}	0.38 ± 0.01^{b}	0.38 ± 0.00^{b}
	TD (g ml^{-1})	0.56 ± 0.01^{d}	0.55 ± 0.01^{d}	0.55 ± 0.01^{d}	0.50 ± 0.02^{e}	0.59 ± 0.00^{c}	0.55 ± 0.01^{d}	0.59 ± 0.01^{c}	0.62 ± 0.01^{b}	0.64 ± 0.02^{b}	0.65 ± 0.02^{b}
	L^*	39.05 ± 0.04^{e}	40.07 ± 0.46^{d}	40.27 ± 0.95^{d}	41.13 ± 0.07^{c}	41.76 ± 0.07^{b,c}	41.86 ± 0.02^{b,c}	41.91 ± 0.63^{b,c}	42.11 ± 0.35^{b}	43.09 ± 0.67^{a}	43.10 ± 0.54^{a}
	a^*	2.74 ± 0.10^{a}	2.81 ± 0.07^{a}	2.77 ± 0.16^{a}	2.58 ± 0.03^{b,c}	2.74 ± 0.02^{a}	2.73 ± 0.03^{a}	2.57 ± 0.01^{c}	2.76 ± 0.05^{a}	2.70 ± 0.09^{a,b}	2.53 ± 0.02^{c}
	b^*	11.58 ± 0.08^{e}	11.91 ± 0.29^{c}	11.65 ± 0.10^{d,e}	11.61 ± 0.01^{d,e}	12.79 ± 0.15^{a}	12.73 ± 0.07^{a}	12.46 ± 0.10^{b}	12.25 ± 0.01^{b}	11.97 ± 0.05^{c}	11.85 ± 0.21^{c,d}
	ΔE	—	1.09 ± 0.49^{d}	1.25 ± 0.92^{c,d}	2.08 ± 0.07^{c}	2.97 ± 0.01^{b}	3.03 ± 0.01^{b}	3.00 ± 0.63^{b}	3.14 ± 0.34^{b}	4.06 ± 0.66^{a}	4.07 ± 0.54^{a}
Functional properties	WAC (g g^{-1})	9.17 ± 0.14^{f}	9.29 ± 0.10^{f}	9.39 ± 0.09^{f}	9.21 ± 0.25^{f}	11.68 ± 0.05^{b}	12.16 ± 0.25^{a}	10.76 ± 0.15^{c}	10.83 ± 0.02^{c}	10.21 ± 0.09^{d}	9.91 ± 0.08^{e}
	OAC (g g^{-1})	0.72 ± 0.02^{e}	0.61 ± 0.04^{f}	0.67 ± 0.03^{e,f}	1.31 ± 0.02^{b}	1.21 ± 0.05^{c}	1.53 ± 0.07^{a}	1.02 ± 0.07^{d}	1.37 ± 0.02^{b}	0.97 ± 0.02^{d}	0.74 ± 0.02^{e}
	EC (%)	25.80 ± 0.61^{e}	26.45 ± 0.07^{d}	28.30 ± 0.04^{c}	25.83 ± 0.24^{e}	29.10 ± 0.42^{b}	30.42 ± 0.12^{a}	26.14 ± 0.22^{d,e}	26.10 ± 0.12^{d,e}	25.10 ± 0.12^{f}	22.11 ± 0.11^{g}
	ES (%)	21.82 ± 0.12^{b}	21.39 ± 0.67^{b,c}	21.39 ± 0.67^{c,d,e}	20.85 ± 0.17^{e,f}	26.10 ± 0.16^{a}	26.10 ± 0.03^{a}	20.52 ± 0.64^{d,e,f}	21.17 ± 0.17^{b,c,d}	20.50 ± 0.38^{d,e,f}	19.84 ± 0.98^{f}
Gel hydration properties	WAI (g g^{-1})	8.33 ± 0.09^{e}	9.47 ± 0.03^{d}	12.07 ± 0.09^{b}	12.12 ± 0.14^{b}	12.00 ± 0.19^{b}	12.66 ± 0.15^{a}	10.57 ± 0.14^{c}	8.13 ± 0.07^{f}	7.98 ± 0.19^{f}	7.37 ± 0.09^{g}
	WSI (g g^{-1})	0.52 ± 0.11^{f}	1.33 ± 0.39^{c,d}	2.18 ± 0.12^{a}	1.40 ± 0.08^{b,c}	1.21 ± 0.05^{c,d,e}	2.18 ± 0.05^{a}	1.10 ± 0.16^{d,e}	1.97 ± 0.10^{a}	0.95 ± 0.04^{b}	0.90 ± 0.07^{e}
	SP (g g^{-1})	6.20 ± 0.13^{e}	10.35 ± 0.04^{d}	12.92 ± 0.10^{a}	11.63 ± 0.06^{b}	10.55 ± 0.07^{c}	11.7 ± 0.18^{b}	9.34 ± 0.09^{e}	7.85 ± 0.06^{f}	6.60 ± 0.17^{g}	6.30 ± 0.04^{e}

[a] Data are presented as a mean value ± standard deviation. Values followed by different superscript letters in each column are significantly different ($p \leq 0.05$). T1: 10 kV – 10 min, T2: 10 kV – 20 min, T3: 10 kV – 30 min, T4: 20 kV – 10 min, T5: 20 kV – 20 min, T6: 20 kV – 30 min, T7: 30 kV – 10 min, T8: 30 kV – 20 min, T9: 30 kV – 30 min. BD – bulk density; TD – tapped density; WAC – water absorption capacity; OAC – oil absorption capacity; SC – swelling capacity; EC – emulsion capacity; ES – emulsion stability; WAI – water absorption index; WSI – water solubility index; SP – swelling power.

kV – 20 min). Further enhancement of exposure time and voltage level significantly decreases the WAI to a lowest value (7.37 g g^{-1}) observed at the highest voltage and time (30 kV – 30 min). The WAI of chia seed flour varies depending on the action of reactive species, affecting the soluble fiber, mucilage, and proteins in the matrix. Plasma etching causes depolymerization of polysaccharides and alters the polar groups of proteins by increasing the number of active sites for water absorption, thus enhancing the WAI in treated flour.[46]

Similarly, CPT was also observed to have a significant ($p \leq 0.05$) influence on the water solubility index (WSI) of chia seed flour that follows the same pattern as for WAC. The WSI was observed to be lowest in the control sample (0.52 g g^{-1}) while the highest value (2.18 g g^{-1}) was observed in treatments T2 and T5. At lower plasma voltage levels (10 and 20 kV), the WSI was also observed to initially increase upon increasing the exposure time to 20 min which thereafter reduced significantly at 30 min. However, at 30 kV plasma treatment, a decreasing WSI value was observed upon increasing the exposure time. Reactive species generated during CPT induce molecular degradation and fragmentation of amorphous and crystalline structures. The reduced crystallinity makes the polar functional groups of polysaccharides readily accessible, which ultimately leads to increased solubility.[40,46] The decline in WSI after extended exposure time to CPT may be due to protein denaturation.[47] High WSI allows easy reconstitution in water or milk with a smooth texture desirable in product formulations like instant soups.[49]

The swelling power (SP) of chia seed flour samples followed a similar trend to that for WSI and CPT samples, which showed better SP than that of the control sample. The SP was found to be the highest (12.92 g g^{-1}) in T2 (10 kV – 20 min). In general, the SP value was observed to initially increase upon increasing the voltage from 10 kV to 20 kV but then significantly ($p \leq 0.05$) reduced upon enhancing the voltage to 30 kV. Further, at lower voltage levels of 10 to 20 kV, SP was observed to initially increase upon increasing the treatment exposure time from 10 to 20 min and then reduced at 30 min. However, at the highest voltage level, the SP significantly ($p \leq 0.05$) decreased with time. A similar trend was reported by Joy *et al.* (2022) in plasma-treated jackfruit seed flour.[26]

3.3 Effect of CPT on the nutritional composition of chia seed flour

3.3.1 Proximate composition. The proximate composition and energy values of chia seed flour samples were significantly ($p \leq 0.05$) influenced by CPT, as shown in Table 2. The moisture content of the control sample was 6.69%, which decreased to 5.81% in sample T9 (30 kV – 30 min). This reduction can be attributed to the plasma etching process, which induces the formation of microscopic pits and pores on the surface, thereby increasing the specific surface area and enhancing the diffusion and evaporation of moisture.[26] Additionally, the reduction in moisture content may also result from the formation of free radicals ($O^{\bullet}$) and ($H^{\bullet}$) through the lysis of surface-bound water molecules.[23,29,45,50] The protein content of the control

samples was measured at 22.84%, while the protein content of the treated samples ranged from 24.63% (T4) to 22.97% (T6). At the lowest voltage level (10 kV), the protein content decreased from 10 to 20 min of exposure, but then increased at 30 min of exposure. However, for 20 and 30 kV exposure, the protein content was decreased with increasing treatment time from 10 to 30 minutes, while comparable results were observed for samples T1 and T8. Plasma treatment influences the protein content by the action of reactive species, either by degradation or aggregation.[22,29] The enhancement can be attributed to the action of reactive species generated by cold plasma induced partial unfolding of protein molecules, exposing the hydrophilic amino acid side chains and thereby improving protein solubility. These structural changes caused by surface etching increase the surface area of the flour matrix, enabling better solvent diffusion and mass transfer, which improves protein extractability.[51] Moreover, chemical modifications, such as oxidation of aromatic rings and amino acid side chains, cleavage of disulfide bonds, and changes in secondary and tertiary structures, further enhance its solubility and extractability.[32,52,53] However, extending the exposure time at higher voltage levels resulted in reduced protein content. This reduction was mainly attributed to the generation of RONS during CPT, which intensifies with increasing treatment time.[52] These reactive species oxidize and break down susceptible amino acids, particularly those containing aromatic and sulphur groups, leading to the cleavage of peptide bonds and the fragmentation of large peptides into smaller, free amino acids. Prolonged exposure promotes cross-linking, which reduces the surface sulfhydryl groups and further lowers detectability.[21,54] Moreover, chemical modifications such as hydroxylation, sulfonation, and nitration disrupt the protein's secondary and tertiary structure, causing aggregation and loss of solubility.[55,56] The reduction in protein content due to higher treatment dosage has been reported by Kheto *et al.* (2023) and Lokeshwari *et al.* (2021) in guar seed flour and pearl millet flour, respectively.[25,40] As shown in Table 2, the ash content of the treated flour samples was significantly higher than that of the control sample, which measured 4.95%. However, comparable results were observed for most treatments, except for samples T6, T8, and T9. The variations in ash content may be explained by two phenomena: (i) the degradation of organic matter in CPT-treated samples resulting in a higher relative concentration of minerals, and (ii) the interaction of the food matrix with the CPT-induced reactive species leading to release of bound minerals or formation of new mineral components.[32] The fat content also varied with the change in the CPT dose. The control sample, having 30.15% of fat, was increased to a peak value of 36.99% in T4 (20 kV – 10 min). At lower voltage (10 kV), the fat content increased with extended exposure time from 33.73% to 36.18% with an increase in exposure time from 10 to 30 min, respectively. However, the increase in CPT voltage from 20 kV to 30 kV significantly reduced the fat content from 36.99% to 35.26%. The increase in fat content at lower voltage might be associated with the moisture loss and disruption of the cellular matrix during the oxidation process driven by hydroxyl and superoxide radicals, leading to the formation of fatty acid derivatives.[25,29,30,40,50] The reductions observed at higher plasma exposure were likely due to the formation of complex compounds generated by the intensified effects of RONS that stimulate oxidative degradation, leading to decomposition of lipid molecules.[32,56] The fiber content of the control sample was measured at 28.24%, whereas the highest was observed for samples T1 and T4 (~30.15%). CPT enhanced the fiber content compared to the control sample, but a decline was observed with prolonged exposure times across all voltage levels. This enhancement might be associated with the action of RONS generated by plasma, which interacts with the cell wall surface, altering fiber composition by converting the insoluble fiber into soluble forms.[32,57] This conversion makes fiber more accessible and measurable, thereby increasing the apparent fiber content. On the other hand, the total carbohydrate content showed a marginal decrease across all treatments for treated samples as compared to the control sample. This reduction may be a consequence of oxidative fragmentation of polysaccharides and cleavage of glycosidic linkages due to reactive species generated during treatment, as well as the overall change in other components.[40,50] The observed changes in the proximate

Table 2 Effect of CPT on the nutritional composition of chia seed flour[a]

	Proximate composition (%)							
Samples	Moisture	Ash	Protein	Fat	Fiber	Total carbohydrate	Energy (kcal/100g)	IVPD (%)
Control	6.69 ± 0.04^{a}	4.95 ± 0.03^{e}	22.84 ± 0.03^{h}	30.15 ± 0.04^{g}	28.41 ± 0.02^{g}	35.37 ± 0.09^{a}	504.19	65.92 ± 0.17^{i}
T1	$6.21 \pm 0.01^{b,c}$	5.25 ± 0.03^{a}	23.82 ± 0.03^{e}	33.73 ± 0.05^{f}	30.15 ± 0.03^{a}	$30.99 \pm 0.11^{b,c}$	522.81	67.95 ± 0.13^{h}
T2	$6.14 \pm 0.04^{c,d}$	$5.20 \pm 0.02^{a,b}$	22.97 ± 0.05^{g}	34.42 ± 0.03^{e}	29.82 ± 0.04^{b}	31.26 ± 0.03^{b}	526.70	68.54 ± 0.15^{f}
T3	6.23 ± 0.01^{b}	5.26 ± 0.02^{a}	24.10 ± 0.09^{c}	36.18 ± 0.03^{b}	28.76 ± 0.04^{e}	28.23 ± 0.11^{g}	534.94	68.09 ± 0.17^{g}
T4	$5.93 \pm 0.02^{f,g}$	$5.22 \pm 0.02^{a,b}$	24.63 ± 0.06^{a}	36.99 ± 0.10^{a}	30.14 ± 0.03^{a}	27.24 ± 0.10^{h}	540.39	72.68 ± 0.09^{a}
T5	5.90 ± 0.01^{g}	5.25 ± 0.04^{a}	24.25 ± 0.07^{b}	35.36 ± 0.09^{c}	29.15 ± 0.02^{c}	29.25 ± 0.11^{f}	532.24	72.57 ± 0.11^{b}
T6	6.12 ± 0.02^{d}	5.08 ± 0.06^{d}	23.97 ± 0.07^{d}	$34.59 \pm 0.03^{d,e}$	28.94 ± 0.03^{d}	30.25 ± 0.17^{d}	528.19	69.46 ± 0.09^{e}
T7	6.02 ± 0.03^{e}	5.26 ± 0.03^{a}	$24.19 \pm 0.05^{b,c}$	35.26 ± 0.03^{c}	29.18 ± 0.03^{c}	29.27 ± 0.09^{f}	531.18	71.93 ± 0.05^{c}
T8	$5.99 \pm 0.01^{e,f}$	$5.18 \pm 0.02^{b,c}$	23.86 ± 0.04^{e}	$35.14 \pm 0.05^{c,d}$	28.65 ± 0.03^{f}	$29.84 \pm 0.08^{d,e}$	531.06	71.83 ± 0.15^{c}
T9	5.81 ± 0.11^{h}	5.13 ± 0.03^{c}	23.65 ± 0.06^{f}	$35.01 \pm 0.02^{c,d,e}$	28.24 ± 0.04^{h}	$30.40 \pm 0.14^{c,d}$	531.29	71.68 ± 0.14^{d}

[a] Data are presented as a mean value ± standard deviation. Values followed by different superscript letters in each column are significantly different ($p \leq 0.05$). T1: 10 kV – 10 min, T2: 10 kV – 20 min, T3: 10 kV – 30 min, T4: 20 kV – 10 min, T5: 20 kV – 20 min, T6: 20 kV – 30 min, T7: 30 kV – 10 min, T8: 30 kV – 20 min, T9: 30 kV – 30 min.

values of flour significantly affected the energy values, which varied from 504.19 kcal/100 g in the control to 540.39 kcal/100 g in sample T4 (20 kV – 10 min). These results suggest that CPT significantly affected the composition of chia seed flour.

3.3.2 Mineral profile. The mineral content of chia seed flour was significantly ($p \leq 0.05$) influenced by the voltage and exposure time of CPT (Table 3). The control sample had 642.59 mg/100 g of calcium (Ca), 497.42 mg/100 g of magnesium (Mg), 582.34 mg/100 g of potassium (K), 757.87 mg/100 g of phosphorus (P), 10.32 mg/100 g of iron (Fe), 6.43 mg/100 g of zinc (Zn), 1.71 mg/100 g of copper (Cu), and 2.88 mg/100 g of manganese (Mn). At the treatment level T2 (10 kV – 20 min), the maximum increase in Ca, Mg, K, Fe, Cu, and Mn content was observed. However, the highest levels of P and Zn were observed for treatment T4 (20 kV – 10 min). At 30 kV plasma exposure, the mineral content increased initially but dropped as the treatment time increased up to 30 min. It is to be noted that across all treatment levels, a substantial decrease in mineral content was observed with an increase in treatment time, indicating the adverse effects of prolonged plasma exposure. The enhanced mineral content at lower and moderate treatment levels is linked to the breakdown of antinutritional factors by plasma, which increases the availability of bound minerals. The findings align with the previously reported studies by Das *et al.* (2025), who observed similar results for Ca, Fe, and Zn content of groundnuts upon plasma exposure. While most of the elements showed an upward trend after CPT, there was, however, a noticeable drop in the Fe content.[53] The reduction in Fe content is due to the reaction of reactive species with the metal ions during plasma exposure, as observed by Zhang *et al.* (2024).[45] In contrast, Charu *et al.* (2024) reported an increase in Fe content, but a reduction in Ca, P, and Mg contents of millets post CPT.[58] The increase in the content of these elements was attributed to the ability of CPT to enhance their bioavailability and accessibility. Hence, it should be noted that optimizing the plasma treatment parameters is essential to significantly improve the nutritional composition of flour, as it can both increase or lower the levels of bioavailable minerals.

3.3.3 *In vitro* protein digestibility. As presented in Table 2, the control sample exhibited the lowest digestibility (65.92%), while the highest value (72.68%) was observed in the T4 sample (20 kV – 10 min), suggesting that CPT can significantly improve ($p \leq 0.05$) the protein digestibility in the treated flour samples. The observed enhancement can be attributed to the action of reactive species generated during CPT, which induce structural modification such as protein unfolding and alteration of amino acid side chains. These modifications expose the previously buried cleavage sites, making them more accessible for proteolysis and thereby enhancing digestibility.[21,52,59] Furthermore, the treatment promotes stretching and partial cleavage of intermolecular bonds within polypeptide chains, facilitating enzyme accessibility. In addition, oxidation of anti-nutritional factors by reactive species may further contribute to improved protein digestibility.[51] Similar observations with enhanced protein digestibility after plasma treatment have been reported by Kheto *et al.* (2023), Patra *et al.* (2024), and Jamali *et al.* (2025).[30,32,40] However, a reduction was observed across all voltage levels at prolonged exposure due to the conformational changes triggered by the reactive species on the peptide bonds of amino acids. This leads to protein denaturation, which disrupts disulfide linkages and subsequently results in protein fragmentation and loss of native structure. The formation of protein fragments due to excessive exposure to reactive species leads to protein aggregation through hydrophobic interactions and covalent cross-linking, thereby reducing protein solubility and enzyme accessibility.[52,55,60] These combined effects inhibit enzymatic hydrolysis, thereby decreasing digestibility after prolonged exposure to cold plasma. Optimal treatment duration is thus critical to balancing protein unfolding and preventing adverse aggregation or degradation. Reduction in IVPD value at higher plasma exposure has been reported by Pal *et al.* (2016) in rice flour.[61]

3.3.4 Total phenolic content (TPC), total flavonoid content (TFC), and antioxidant activity (AOA). Bioactive compounds are found abundantly in plant foods, offering various nutritional and health-promoting effects, including reduced risk of oxidative stress and metabolic diseases. Phenolic compounds are

Table 3 Effect of CPT on the mineral content of chia seed flour[a]

	Mineral profile (mg/100g)							
Samples	Ca	Mg	K	P	Fe	Zn	Cu	Mn
Control	642.59 ± 1.47^{e}	497.42 ± 1.28^{d}	582.34 ± 0.67^{e}	757.87 ± 1.29^{j}	$10.32 \pm 0.54^{a,b}$	$6.43 \pm 0.27^{a,b,c}$	1.71 ± 0.61^{c}	$2.88 \pm 0.32^{b,c}$
T1	639.30 ± 1.25^{f}	472.46 ± 0.93^{f}	555.51 ± 1.39^{h}	800.93 ± 1.04^{e}	9.52 ± 0.55^{c}	$6.24 \pm 0.13^{b,c}$	1.77 ± 0.29^{c}	$2.75 \pm 0.38^{b,c}$
T2	827.25 ± 1.02^{a}	610.59 ± 0.65^{a}	696.69 ± 1.03^{a}	902.91 ± 1.90^{c}	10.68 ± 0.29^{a}	$6.26 \pm 0.54^{b,c}$	2.75 ± 0.22^{a}	4.48 ± 0.44^{a}
T3	585.46 ± 1.28^{i}	448.33 ± 1.08^{i}	547.56 ± 1.07^{j}	771.63 ± 0.68^{h}	8.30 ± 0.42^{d}	$6.33 \pm 0.22^{a,b,c}$	1.70 ± 0.34^{c}	2.16 ± 0.26^{c}
T4	732.71 ± 0.94^{c}	560.30 ± 1.09^{c}	655.66 ± 0.71^{c}	954.00 ± 1.34^{a}	$10.19 \pm 0.47^{a,b}$	7.12 ± 0.57^{a}	$2.10 \pm 0.10^{a,b,c}$	3.29 ± 0.50^{b}
T5	582.73 ± 1.21^{j}	441.54 ± 0.68^{j}	550.47 ± 0.59^{i}	764.99 ± 0.68^{i}	8.43 ± 0.34^{d}	$7.03 \pm 0.49^{a,b}$	1.58 ± 0.42^{c}	2.35 ± 0.58^{c}
T6	609.36 ± 1.40^{g}	468.63 ± 0.60^{g}	568.99 ± 1.04^{f}	794.17 ± 1.72^{f}	7.27 ± 0.62^{e}	6.20 ± 0.39^{c}	$1.84 \pm 0.44^{b,c}$	$2.90 \pm 0.31^{b,c}$
T7	648.75 ± 0.45^{d}	482.43 ± 1.24^{e}	588.20 ± 1.01^{d}	802.52 ± 1.15^{d}	7.78 ± 0.37^{e}	$6.41 \pm 0.20^{a,b,c}$	1.66 ± 0.27^{c}	2.41 ± 0.48^{c}
T8	772.48 ± 1.04^{b}	596.10 ± 0.85^{b}	671.25 ± 1.09^{b}	906.57 ± 1.85^{b}	7.95 ± 0.68^{e}	7.15 ± 0.77^{a}	$2.59 \pm 0.11^{a,b}$	3.45 ± 0.24^{b}
T9	602.13 ± 1.01^{h}	460.46 ± 1.37^{h}	559.50 ± 1.03^{g}	782.15 ± 0.97^{g}	7.39 ± 0.39^{e}	$6.71 \pm 0.19^{a,b}$	1.71 ± 0.85^{c}	2.43 ± 0.30^{c}

[a] Data are presented as a mean value ± standard deviation. Values followed by different superscript letters in each column are significantly different ($p \leq 0.05$). T1: 10 kV – 10 min, T2: 10 kV – 20 min, T3: 10 kV – 30 min, T4: 20 kV – 10 min, T5: 20 kV – 20 min, T6: 20 kV – 30 min, T7: 30 kV – 10 min, T8: 30 kV – 20 min, T9: 30 kV – 30 min.

natural antioxidants that inhibit the activity of free radicals and possess strong antioxidant, anticarcinogenic, and antimutagenic properties.[46] The total phenolic content (TPC) was significantly ($p \leq 0.05$) affected by applied voltage level and time duration (Fig. 2a). In the present study, the control sample exhibited the lowest TPC value of 0.8 mg GAE per g, whereas all CP-treated samples showed a significant enhancement, with the highest TPC value (1.68 mg GAE per g) recorded for T4 (20 kV – 10 min). This increase may be attributed to the plasma-induced oxidative stress, which is known to stimulate the release of secondary metabolites, including phenolics.[23,30] However, a slight decline in TPC was observed beyond T4 (20 kV – 10 min), which could be linked to the potential degradation of sensitive phenolic components in the flour upon prolonged or higher intensity plasma exposure. Prolonged exposure to high-intensity plasma treatment can accelerate the oxidative reactions, breaking the aromatic benzene rings and aliphatic side chains, which degrade the phenolic structure.[46] Similar findings have been reported by Sarangapani *et al.* (2016), Patra *et al.* (2024), and Amiri *et al.* (2023) for plasma-treated parboiled rice flour, horse gram flour, and buckwheat flour, respectively.[23,30,62]

Total flavonoid content (TFC) followed a similar trend (Fig. 2b), with the maximum value (0.62 mg per QE g) observed at T4 (20 kV – 10 min), while the control sample exhibited the lowest flavonoid content (0.49 mg per QE g). The rise in TFC can be attributed to the depolymerization of polysaccharides and enhanced release of bound flavonoid compounds. Furthermore, moderate plasma exposure may have stimulated phenylalanine ammonia-lyase enzyme activity, thereby enhancing the biosynthesis of flavonoids.[23,63] However, at moderate (20 kV) and higher (30 kV) voltages, a decline in flavonoid content was observed with increasing exposure time. This might be due to the oligomerization of polyphenolic compounds, resulting from the scavenging reaction with reactive species.[20] Likewise, Kheto *et al.* (2023) and Sarkar *et al.* (2023) have reported a reduction in TFC content at higher plasma exposure.[29,40]

Antioxidant activity (Fig. 2c) also improved with plasma treatment, reaching its maximum (58.36%) at T4 (20 kV – 10 min). This trend coincides with the increase in TPC and TFC, supporting their role in scavenging free radicals. However, AOA declined slightly under extended treatment conditions, indicating that antioxidant compounds may degrade at higher treatment levels. In general, our findings match the previously reported studies by Kheto *et al.* (2023), Sarkar *et al.* (2023), and Patra *et al.* (2024).[29,30,40]

3.3.5 Antinutritional factors. Antinutritional factors, such as tannins and phytates, are secondary metabolites naturally developed in seeds to defend against environmental pathogens. However, their presence at high concentrations can hinder mineral bioavailability and reduce *in vitro* protein digestibility by forming complexes with dietary proteins and essential minerals. As shown in Fig. 2d, total tannin content (TTC) in the control sample was recorded at 3.48 mg TAE per g. CPT significantly ($p \leq 0.05$) influenced the TTC across all treatment conditions, with a notable reduction (2.88 mg TAE per g) observed at T6 (20 kV – 30 min). The declining trend across all treatment voltages was observed with increasing exposure time

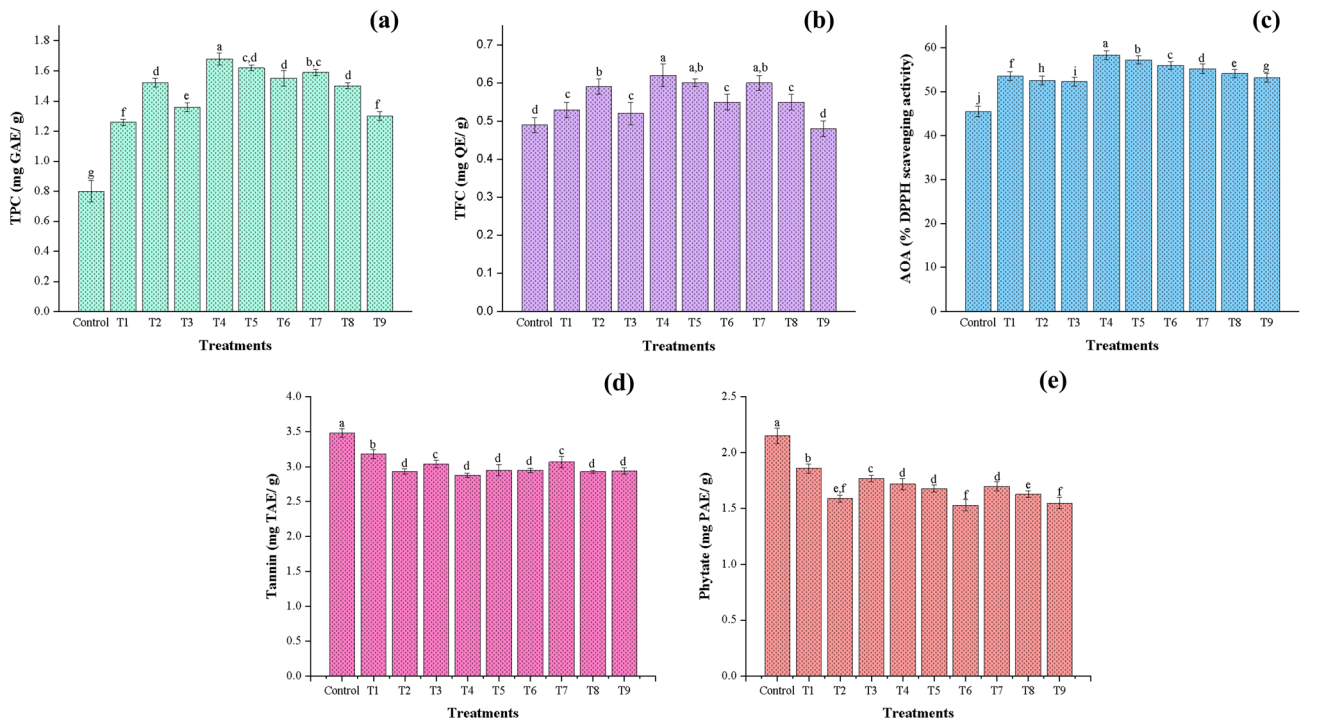

Fig. 2 Effect of CPT on the antioxidant and antinutrient components of chia seed flour: (a) total phenolic content, (b) total flavonoid content, (c) antioxidant activity, (d) phytate content, and (e) tannin content under different treatment conditions. All column bars and error bars are stated as mean ± standard deviations ($p \leq 0.05$). T1: 10 kV – 10 min, T2: 10 kV – 20 min, T3: 10 kV – 30 min, T4: 20 kV – 10 min, T5: 20 kV – 20 min, T6: 20 kV – 30 min, T7: 30 kV – 10 min, T8: 30 kV – 20 min, T9: 30 kV – 30 min.

from 10 to 30 min. This reduction in TTC may be due to the action of RONS on the polyphenolic compounds, turning them into simpler structures upon oxidation, degrading the glycosidic linkages, and causing the cleavage of phosphate-phenolic bonds, thereby disrupting their chemical integrity. Similar reductions in TTC content were reported in CP-treated pearl millet flour,[29] guar seed flour[40] and horse gram flour.[30] Phytates, also called phytic acid or myo-inositol hexa-phosphate, account for 1–5% of phosphorus by weight in cereals, legumes, and oilseeds. Owing to their negatively charged structure, they form insoluble complexes with essential minerals such as calcium, magnesium, and zinc, thereby hindering their bioavailability. From Fig. 2e, CPT significantly reduced the phytate content of chia seed flour, and followed a similar trend to that of tannin content. The phytate content of the control sample was 2.15 mg PAE per g, and the maximum reductions were observed in sample T6 (20 kV – 30 min), *i.e.*, 1.53 mg PAE per g, followed by sample T9 (30 kV – 30 min). The prolonged treatment time has more efficiently reduced phytate content by facilitating the breakdown of the phytate ring and enhancing the endogenous activity of the phytase enzyme due to the higher accumulation of RONS, further increasing mineral bioavailability.[64] Reductions in phytate content in plasma-treated flour were also observed by other researchers.[29,30,40]

3.4 Effect of CPT on the pasting properties of chia seed flour

The pasting characteristics of chia seed flour are displayed in Table 4. The pasting properties of the chia seeds are primarily governed by their proteins, dietary fiber, gums, and mucilage, rather than starch gelatinization. The soluble fiber and mucilage fractions swell and form viscous gels, while proteins aid in water absorption, contributing to the development of viscosity.[65] Consequently, chia's peak viscosity and gelation arise from these non-starch components, distinguishing it from conventional starch-rich flours like wheat and corn. The absence of crystalline structure related to amylose and amylopectin in the XRD pattern further validates that starch does not affect the pasting attributes of the treated chia flour. Similar observations were reported by García-Salcedo *et al.* (2018).[42] As observed, the treatment exposure affects peak viscosity and breakdown viscosity more than power levels. The peak viscosity (PV) increased initially until T3 (10 kV – 30 min). Furthermore, an increase in voltage level and time resulted in a reduction in the PV due to the solubilization of the flour component. Viscosity of chia seed flour was enhanced during heating from 80 to 90 °C, and it was characterized by a complex grid of fibers, gums, and proteins. The temperature allows the matrix to trap more water, thus increasing the viscosity. Similar findings were reported by Kaur and Annapure (2023).[28] Meanwhile, the cooling cycle from 90 °C to 50 °C causes syneresis, resulting in a decrease in the viscosity of the samples. An increase in breakdown viscosity was observed at T3 (10 kV – 30 min) with a maximum value of 1034 (cP) as compared to the control sample, *i.e.*, 430.6 (cP), also referred to as the trough viscosity, which helps to maintain the peak viscosity of the paste. This indicates that the flour has low stability after gelatinization.[26] These changes are in accordance with the swelling properties and decreased crystallinity of treated chia seed flour, which significantly affected the pasting properties. Various other flours, such as little millet flour,[27] pearl millet flour[25] and wheat flour,[24] have been examined for their pasting behaviour, revealing similar findings upon CPT.

3.5 Effect of CPT on the thermal properties of chia seed flour

The thermal properties of control and CPT flour samples are presented in Table 4. CPT significantly ($p \leq 0.05$) influenced the thermal behaviour of chia seed flour, with variations observed across different voltages and exposure durations. The control sample exhibited the lowest onset (T_o) – 100 °C, peak (T_p) – 114 °C, and conclusion (T_c) – 130 °C temperatures, indicating its native structural integrity and inherent thermal sensitivity. Plasma treatment at T2 (10 kV – 20 min) resulted in the most pronounced enhancement in thermal stability, reflecting the highest peak (133 °C) and end temperatures (142 °C), likely due to molecular rearrangements that enhanced thermal resistance. The observed increase in peak temperatures at certain treatment levels can be attributed to enhanced cross-linking and partial depolymerization, induced by interactions of plasma species with carbohydrates and protein molecules.[27,66] In contrast, treatments at higher voltages (20 and 30 kV) and extended exposure durations (30 min) resulted in reduced T_p and T_c values, suggesting possible structural disruption resulting in degradation of essential macromolecules. A reduction in T_p with increasing exposure time has been observed in guar seed flour[40] and pearl millet flour.[29] These structural modifications are a result of intensified intermolecular interactions promoted by plasma treatment upon action of reactive species.[24,26]

3.6 Effect of CPT on the structural and molecular characterization of chia seed flour

3.6.1 Fourier transform infrared spectroscopy (FTIR). Fig. 3 displays the FTIR spectra of chia seed flour, comparing the control to treated samples at varying voltages and durations. The overall transmittance patterns remain similar across all samples, indicating a consistent trend in transmittance for both the control and the treated samples. This consistent pattern suggests that CPT does not generate new functional groups in chia seed flour. However, distinct changes in peak intensity and broadening were observed among treated samples, particularly as plasma voltage and treatment duration increased. The broad peaks observed around 3281 cm^{-1} were possibly attributed to O–H stretching, 3012 cm^{-1} to C=C–H stretching, and 2925 cm^{-1} to C=H stretching.[47] These peaks suggest the presence of carbohydrates and polysaccharides in chia seed flour. Samples treated at a higher voltage (30 kV) exhibited reduced intensity at 3281 cm^{-1}, suggesting possible changes in intermolecular hydrogen bonding and structural reorganization or cross-linking, which may be attributed to modification, degradation, or interaction of polysaccharides or mucilage during the treatment process.[13,15,27,67] The peak observed at 1744 cm^{-1} corresponds to the ester carbonyl band of terpene alkaloids, which are commonly found in lipids and other organic

Table 4 Effect of CPT on the thermo-pasting properties of chia seed flour[a]

Samples	Thermal properties				Pasting properties				
	T_o (°C)	T_p (°C)	T_c (°C)	PV (cP)	BV (cP)	FV (cP)	SV (cP)	Pt (sec)	PT (°C)
Control	100.60 ± 0.36^{e}	114.63 ± 0.38^{i}	130.70 ± 0.26^{i}	1290.00 ± 0.90^{i}	430.60 ± 0.98^{j}	1061.00 ± 0.98^{b}	229.30 ± 0.85^{j}	310.00 ± 0.50^{c,d}	72.22 ± 0.21^{d}
T1	103.90 ± 0.20^{c}	132.63 ± 0.21^{b}	140.63 ± 0.21^{b}	1418.00 ± 0.93^{h}	538.40 ± 0.45^{i}	973.80 ± 0.82^{g}	443.80 ± 0.91^{h}	312.10 ± 0.76^{a,b}	75.07 ± 0.05^{c}
T2	104.73 ± 0.21^{b}	133.50 ± 0.30^{a}	142.57 ± 0.25^{a}	1637.00 ± 1.03^{e}	715.10 ± 0.67^{e}	968.60 ± 0.89^{h}	668.60 ± 0.80^{e}	313.20 ± 0.42^{a}	75.38 ± 0.10^{b}
T3	103.60 ± 0.36^{c}	128.67 ± 0.21^{d}	137.57 ± 0.31^{d}	1899.00 ± 0.91^{a}	1034.00 ± 0.62^{a}	859.60 ± 0.87^{j}	1040.00 ± 0.70^{a}	313.70 ± 0.25^{a}	59.99 ± 0.05^{i}
T4	104.53 ± 0.35^{b}	123.63 ± 0.25^{f}	136.43 ± 0.35^{e}	1815.00 ± 0.87^{b}	882.90 ± 0.92^{b}	1015.00 ± 0.65^{e}	800.10 ± 0.49^{b}	310.00 ± 0.10^{d}	78.11 ± 0.05^{a}
T5	103.53 ± 0.31^{c}	130.43 ± 0.31^{c}	139.60 ± 0.20^{c}	1510.00 ± 1.00^{g}	566.80 ± 0.77^{h}	1101.00 ± 0.96^{a}	409.10 ± 0.45^{i}	311.90 ± 040^{c}	60.83 ± 0.02^{h}
T6	102.47 ± 0.31^{d}	118.90 ± 0.10^{h}	131.43 ± 0.12^{h}	1703.00 ± 0.89^{d}	691.80 ± 0.82^{f}	1038.00 ± 0.92^{c}	665.70 ± 0.51^{f}	313.80 ± 0.30^{a}	64.74 ± 0.28^{e}
T7	107.97 ± 0.31^{a}	126.53 ± 0.32^{e}	134.33 ± 0.23^{f}	1801.00 ± 0.94^{c}	826.10 ± 0.89^{c}	1024.00 ± 0.72^{d}	776.90 ± 0.95^{h}	313.40 ± 0.30^{a}	55.91 ± 0.06^{j}
T8	107.57 ± 0.21^{a}	120.40 ± 0.20^{g}	132.13 ± 0.25^{g}	1702.00 ± 0.90^{d}	759.50 ± 0.68^{d}	944.70 ± 0.81^{i}	757.70 ± 0.85^{e}	313.10 ± 0.15^{a}	62.14 ± 0.03^{g}
T9	104.63 ± 0.31^{b}	119.07 ± 0.25^{h}	132.47 ± 0.32^{g}	1558.00 ± 1.01^{f}	635.90 ± 0.99^{g}	987.50 ± 0.90^{h}	570.30 ± 0.68^{g}	311.40 ± 0.15^{c}	62.39 ± 0.01^{f}

[a] Data are presented as a mean value ± standard deviation. Values followed by different superscript letters in each column are significantly different ($p \leq 0.05$). T1: 10 kV – 10 min, T2: 10 kV – 20 min, T3: 10 kV – 30 min, T4: 20 kV – 10 min, T5: 20 kV – 20 min, T6: 20 kV – 30 min, T7: 30 kV – 10 min, T8: 30 kV – 20 min, T9: 30 kV – 30 min. T_o – onset temperature; T_p – peak temperature; T_c – conclusion temperature; PV – peak viscosity, BV – breakdown viscosity; FV – final viscosity; SV – setback viscosity; Pt – peak time; PT – pasting temperature.

Fig. 3 FTIR spectra of control and cold plasma-treated chia seed flour samples.

compounds. The transmittance intensity increased in 20 kV-treated samples; however, it decreased for 30 kV-treated samples. The change in intensities of the treated samples in this region indicates modifications to the lipid structures, as oxidation from plasma forms new carbonyl groups, resulting in increased C=O peak intensities as the treatment voltage and time increase. The bands at 1546 cm^{-1} and 1245 cm^{-1} confirm the presence of phenolic (C–O) groups associated with tocopherols.[42,68] The peaks around 1640 cm^{-1} may be ascribed to the amide-I group (secondary structure), and peaks around 1653 cm^{-1} to 1455 cm^{-1} are associated with the N–H bonds of the amide II groups.[69] Compared to the control, the FTIR spectra of the treated samples exhibited higher transmittance with increasing CPT doses, and a change in intensity in the amide region, indicating alterations in the protein secondary structure. However, a gradual decrease, especially in the T6–T9 range of the amide-II region, may be due to the substantial unfolding and fragmentation of peptide bonds and C–N/N–H linkages at higher voltages and time durations. The peaks detected around 1490–1458 cm^{-1} were due to the stretching of the carboxyl group of uronic acids.[70] The peak identified at 1458 cm^{-1} indicates the presence of $-CH_3$ groups and C=C bonds, suggesting the presence of unsaturated fatty acids.[71] The variations observed in this region among treated samples are possibly due to changes in the lipid backbone structures. The peaks detected at 1245 cm^{-1} and 1155 cm^{-1} were attributed to the presence of (N–H) amide III and bending vibrations of the pyranose ring, respectively. The bands detected at around 1045 cm^{-1} represented the C–O–C stretching and C–O–H bending, associated with polysaccharide compounds.[13,42,70] The changes observed in the peak intensities of the FTIR spectra indicate that CPT induces significant alterations in the molecular structure and composition of treated flour samples, which potentially lead to changes in the functional and nutritional properties of the flour.

3.6.2 X-ray diffraction (XRD). Fig. 4 illustrates the X-ray diffractogram of treated flour samples. The broad diffused peaks represent the amorphous region of the sample, while the two sharp peaks observed at 2θ angles of 15° and 30° represent

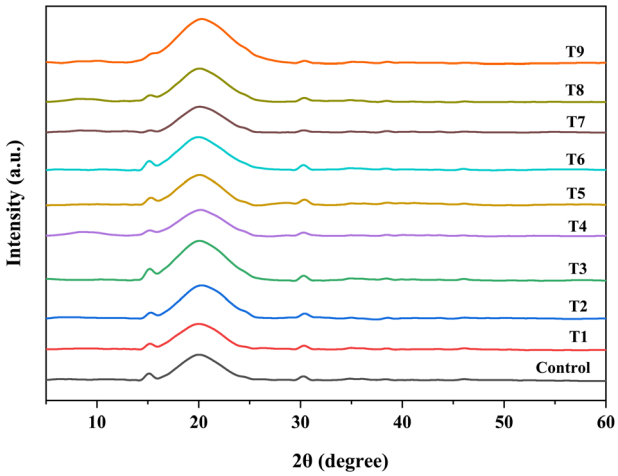

Fig. 4 X-ray diffraction patterns of control and cold plasma-treated chia seed flour samples.

the crystalline structure. García-Salcedo *et al.* (2018) reported similar peaks for chia seed flour and its mucilage, identifying them as magnesium hydrogen phosphate hydrate and calcium carbonate using the powder diffraction file.[42] The enhanced mineral content of Ca, Mg, and P (Table 1) confirms the presence of these elements in the flour matrix. No significant peak shifting was observed in the crystalline areas on varying the treatment conditions of cold plasma-treated flour samples. However, with the increase in treatment conditions, the crystallinity of chia seed flour decreased from 3.24% in the control sample to a minimum of 1.18% in T7 (30 kV – 10 min). Similar results have been reported by other researchers, who observed a decrease in crystallinity in treated samples, such as jackfruit seed flour[26] and wheat flour.[24]

3.6.3 Scanning electron microscopy (SEM). The morphological effects of CPT on chia seed flour are illustrated in Fig. 5. The control sample exhibited a dense and compact surface morphology, characterized by smooth, spherical granules with minimal disruption, indicating a well-preserved structural matrix. In contrast, the CP-treated samples exhibited progressive morphological changes with increasing voltage from 10 kV to 30 kV and treatment durations ranging from 10 to 30 min. At lower intensities (10 kV for 10–20 min), the flour particles exhibited moderate surface roughness, with slightly loosened clusters and minor cracks, indicating the onset of surface etching and partial disruption of polymeric interactions. As the intensity and duration increased, significant alterations in the microstructures became evident. These samples displayed more porous and rougher surfaces, as well as a higher degree of fragmentation, with noticeable cracks. The appearance of broken and deformed particles suggests that plasma-induced oxidation, depolymerization, and surface erosion processes have occurred. Such effects are associated with RONS, which accelerate surface etching, reduce crystallinity, and promote molecular reorientation, leading to enhanced hydration.[66,72] Similar results have been reported in previous studies on cold plasma-treated flours such as jackfruit seed flour,[26] quinoa flour,[47] guar seed flour[40] and little millet flour.[27]

3.7 Principal component analysis (PCA)

Fig. 6 presents the PCA biplot, illustrating the correlation between CPT conditions applied to flour samples and their techno-functional, nutritional, antinutritional, and antioxidant properties. The loading vectors (blue lines) represent the various measured parameters, while the score vectors (red dots) correspond to specific treatment conditions. In this figure, PC-1 (61.35%) and PC-2 (17.30%) collectively account for 78.65% of

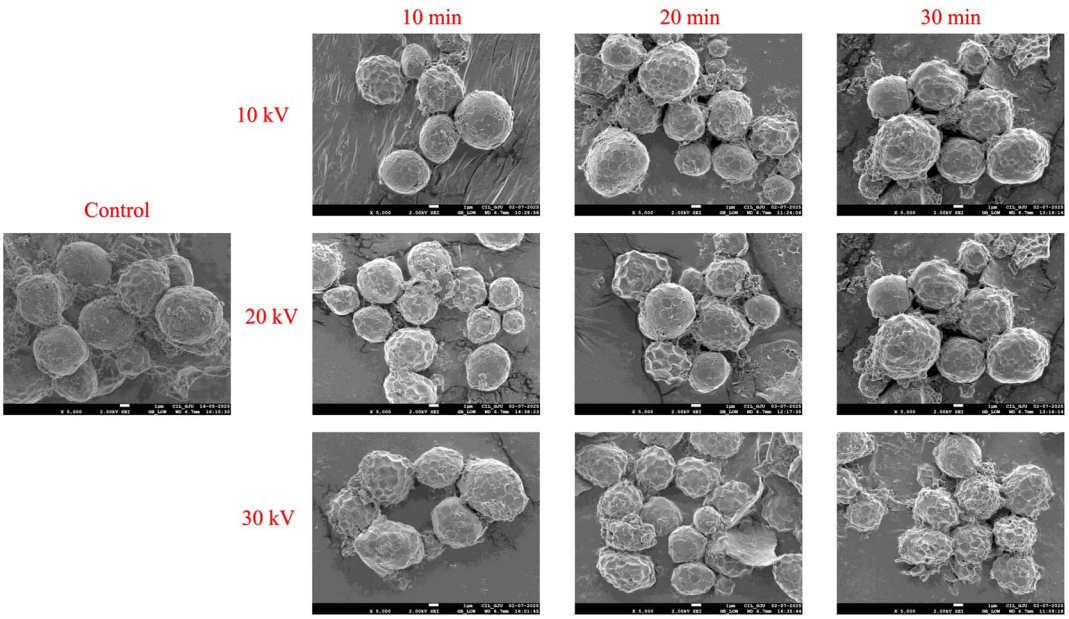

Fig. 5 SEM analysis of control and cold plasma-treated chia seed flour samples.

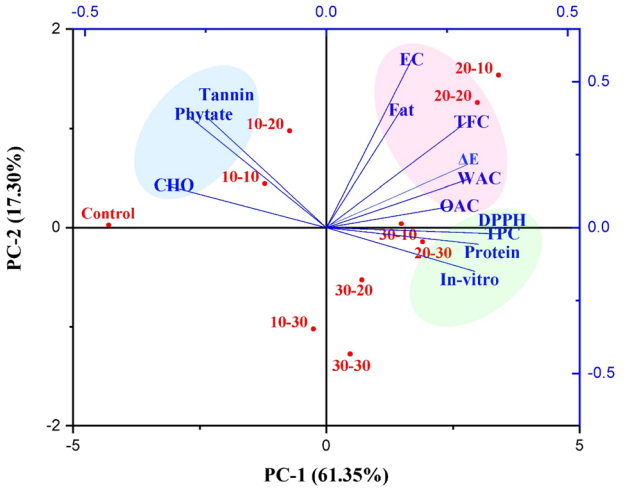

Fig. 6 Principal component analysis of chia seed flour samples.

the total variance, indicating a strong and reliable clustering between treatment conditions. The PCA plot shows that the control and 10 kV samples are closely associated with higher levels of CHO and anti-nutritional factors such as tannins and phytates, located on the negative side of PC-1. This suggests that lower voltage and shorter exposure time had a limited effect on these properties. In contrast, samples treated at 20 kV showed a strong positive association with improved bioactive compounds (TPC, TFC, and DPPH scavenging activity), protein content, and IVPD. These treatments likely generated sufficient ROS to induce favourable modifications in protein structure and antioxidant activity. They also showed enhanced WAC, OAC, and ΔE, suggesting improved techno-functional properties due to structural unfolding and increased exposure of hydrophilic and hydrophobic sites. Treatments clustered towards the centre were positively correlated with increased fat content and EC. Overall, the PCA biplot clearly differentiates between low, medium, and high plasma treatment, showing how these influence the compositional properties of chia seed flour. These findings are also well-supported and validated by thermal (DSC), microstructural (SEM), molecular (FTIR), and crystallinity (XRD) analysis of flour.

4 Conclusion

The present study demonstrated a significant impact ($p \leq 0.05$) of CPT at varying voltages and exposure durations on the nutritional, anti-nutritional, techno-functional, thermal, pasting, and structural properties of chia seed flour. Moderate CP treatment conditions, particularly 20 kV for 10–20 min, enhanced the functional and nutritional properties of chia seed flour. These improvements were attributed to the depolymerization and unfolding of protein and carbohydrate structures, resulting in improved nutrient bioavailability and absorption. Concurrently, a substantial reduction in anti-nutritional factors, such as tannins and phytates, was observed under these conditions. Conversely, treatments at higher intensity (30 kV) resulted in a decline in several key properties, likely due to the degradation of peptide and hydroxyl bonds and the initiation of oxidation reactions. These effects negatively influenced the crystallinity, thermal stability, and microstructure of chia seed flour. Overall, CPT has proven to be a promising non-thermal processing technique that enhances the quality and functionality of chia seed flour, also improving its nutritional integrity. It offers advantages over conventional thermal methods by being energy-efficient, reducing chemical usage, and offering a green alternative. The findings underscore the importance of precise optimization of CP parameters (voltage and exposure time) to tailor flour quality for specific industrial applications, such as bakery, extrusion, or meat products. Future research should aim to investigate molecular-level structural changes using advanced analytical techniques, explore synergistic effects with other emerging processing technologies, and conduct comprehensive shelf-life and formulation studies to broaden the commercial applicability of plasma-treated flours in the food industry.

Author contributions

A. B.– writing – original draft, review & editing, methodology, investigation, formal analysis, data curation, validation. C. S.– methodology & investigation. R. S.– supervision, review & editing. V. S. S. supervision, conceptualization. T. L. S.– writing – review & editing, supervision, conceptualization.

Conflicts of interest

The authors declare that there is no conflict of interest.

Data availability

The data supporting the findings of this research are provided within the article.

Acknowledgements

The authors sincerely thank the National Institute of Food Technology and Entrepreneurship Management (NIFTEM), Kundli, for providing essential resources required for this research. The publication ID for this manuscript from NIFTEM-K is NIFTEM-P-2024-134.

References

1 W. Khalid, M. S. Arshad, A. Aziz, M. A. Rahim, T. B. Qaisrani, F. Afzal, A. Ali, A. Nawaz, M. Z. Khalid and F. M. Anjum, *Food Nutr. Sci.*, 2023, **11**, 3–16.
2 L. A. Muñoz, A. Cobos, O. Diaz and J. M. Aguilera, *Food Rev. Int.*, 2013, **29**, 394–408.
3 N. Vera-Cespedes, L. A. Muñoz, M. Á. Rincón and C. M. Haros, *Foods*, 2023, **12**, 3013.
4 M. Knez Hrnčič, M. Ivanovski, D. Cör and Ž. Knez, *Molecules*, 2019, **25**, 11.
5 A. H. Dinçoğlu and Ö. Yeşildemir, *Curr. Nutr. Food Sci.*, 2019, **15**, 327–337.

6 R. I. M. Almoselhy, A. Usmani and M. A. Siddiqui, *SSRN*, 2025, 1–12.
7 B. Kulczyński, J. Kobus-Cisowska, M. Taczanowski, D. Kmiecik and A. Gramza-Michałowska, *Nutrients*, 2019, **11**, 1242.
8 S. Biswas, F. Islam, A. Imran, T. Zahoor, R. Noreen, M. Fatima, S. M. Zahra and M. A. Shah, *Cogent Food Agric.*, 2023, **9**(1), DOI: **10.1080/23311932.2023.2220516**.
9 S. Motyka, E. Skała, H. Ekiert and A. Szopa, *J. Funct.Foods*, 2023, **103**, 105480.
10 A. B. T. Constantino and E. E. Garcia-Rojas, *J. Sci. Food Agric.*, 2022, **102**, 2630–2639.
11 L. T. B. Sandri, F. G. Santos, C. Fratelli and V. D. Capriles, *Food Nutr. Sci.*, 2017, **5**, 1021–1028.
12 M. A. Gómez-Favela, R. Gutiérrez-Dorado, E. O. Cuevas-Rodríguez, V. A. Canizalez-Román, C. del Rosario León-Sicairos, J. Milán-Carrillo and C. Reyes-Moreno, *Plant Foods Hum. Nutr.*, 2017, **72**, 345–352.
13 M. Hatamian, M. Noshad, S. Abdanan-Mehdizadeh and H. Barzegar, *NFS J.*, 2020, **21**, 1–8.
14 A. M. Abdel-Aty, A. M. Elsayed, H. A. Salah, R. I. Bassuiny and S. A. Mohamed, *Food Sci. Biotechnol.*, 2021, **30**, 723–734.
15 A. Kataria, S. Sharma, A. Singh and B. Singh, *J. Food Meas. Char.*, 2022, **16**, 332–343.
16 K. Miranda-Ramos, Ma. C. Millán-Linares and C. M. Haros, *Foods*, 2020, **9**, 663.
17 M. Mesías, P. Gómez, E. Olombrada and F. J. Morales, *Food Chem.*, 2023, **401**, 134169.
18 A. Haripriya and N. Aparna, *Int. J. Food Nutr. Sci.*, 2018, **3**, 200–206.
19 S. A. Mir, M. A. Shah and M. M. Mir, *Food Bioprocess Technol.*, 2016, **9**, 734–750.
20 N. U. Sruthi, K. Josna, R. Pandiselvam, A. Kothakota, M. Gavahian and A. M. Khaneghah, *Food Chem.*, 2022, (368), DOI: **10.1016/j.foodchem.2021.130809**.
21 B. Kopuk, R. Gunes and I. Palabiyik, *Food Chem.*, 2022, **382**, 132356.
22 R. Thirumdas, R. R. Deshmukh and U. S. Annapure, *J. Food Sci. Technol.*, 2016, **53**, 2742–2751.
23 C. Sarangapani, R. Thirumdas, Y. Devi, A. Trimukhe, R. R. Deshmukh and U. S. Annapure, *LWT–Food Sci. Technol.*, 2016, **69**, 482–489.
24 S. Chaple, C. Sarangapani, J. Jones, E. Carey, L. Causeret, A. Genson, B. Duffy and P. Bourke, *Innov. Food Sci. Emerg. Technol.*, 2020, (66), DOI: **10.1016/j.ifset.2020.102529**.
25 R. Lokeswari, P. S. Sharanyakanth, J. Stephen and R. Mahendran, *IEEE Trans. Plasma Sci.*, 2021, **49**, 1745–1751.
26 J. K. Joy, R. Gracy, G. Eazhumalai, S. P. Kahar and U. S. Annapure, *Innov. Food Sci. Emerg. Technol.*, 2022, **78**, DOI: **10.1016/j.ifset.2022.103009**.
27 S. Jaddu, R. C. Pradhan and M. Dwivedi, *Innov. Food Sci. Emerg. Technol.*, 2022, **77**, DOI: **10.1016/j.ifset.2022.102957**.
28 P. Kaur and U. S. Annapure, *Food Res. Int.*, 2023, **169**, DOI: **10.1016/j.foodres.2023.112930**.
29 A. Sarkar, T. Niranjan, G. Patel, A. Kheto, B. K. Tiwari and M. Dwivedi, *J. Food Process. Eng.*, 2023, **46**, e14317.
30 A. Patra, V. A. Prasath, A. S. Shende, R. Thakur, B. Deep, G. Madhumathi and P. Sarkar, *J. Food Process. Eng.*, 2024, **47**(3), DOI: **10.1111/jfpe.14571**.
31 N. Mollakhalili-meybodi, N. Jamali, M. Sharifian, M. Kiani and A. Nematollahi, *Appl. Food Res.*, 2024, **4**, 100517.
32 N. Jamali, A. Nematollahi, Z. Rahmdar, M. Kiani, M. Torkashvand and N. Mollakhalili-meybodi, *J. Food Process. Preserv.*, 2025, (1), DOI: **10.1155/jfpp/8829261**.
33 S. Mutlu, I. Palabiyik, B. Kopuk, R. Gunes, E. Boluk, U. Bagcı, D. Özmen, O. S. Toker and N. Konar, *Food Biosci.*, 2023, **56**, 103178.
34 S. Ahmadian, F. Sohbatzadeh, F. J. Alashti and R. E. Kenari, *Food Chem.:X*, 2025, **28**, 102574.
35 D. Solanki, I. Oey, S. Prakash, B. Bhandari and J. K. Sahu, *Sustainable Food Technol.*, 2024, **2**, 993–1010.
36 S. K. Pankaj, N. N. Misra, K. J. Alzahrani, A. S. Alamri and C. M. Galanakis, *J. Food Process. Eng.*, 2025, **48**(3), DOI: **10.1111/jfpe.70072**.
37 S. Chandra, S. Singh and D. Kumari, *J. Food Sci. Technol.*, 2014, (1), DOI: **10.1007/s13197-014-1427-2**.
38 AOAC, *Official Methods of Analysis 17th*, 925.10, 992.16, Gaithersburg, MD, USA, 2000.
39 E. Beyzi, A. Gunes, S. Buyukkilic Beyzi and Y. Konca, *Ind. Crops Prod.*, 2019, **129**, 10–14.
40 A. Kheto, A. Mallik, R. Sehrawat, K. Gul and W. Routray, *Food Res. Int.*, 2023, **168**, DOI: **10.1016/j.foodres.2023.112790**.
41 A. Kheto, D. Joseph, M. Islam, S. Dhua, R. Das, Y. Kumar, R. Vashishth, V. S. Sharanagat, K. Kumar and P. K. Nema, *J. Food Process. Preserv.*, 2022, **46**, e16595.
42 Á. J. García-Salcedo, O. L. Torres-Vargas, A. del Real, B. Contreras-Jiménez and M. E. Rodriguez-Garcia, *Food Struct.*, 2018, **16**, 59–66.
43 R. K. Gupta, P. Guha and P. P. Srivastav, *J. Clean. Prod.*, 2024, **461**, 142710.
44 R. Upadhyay, R. Thirumdas, R. R. Deshmukh, U. Annapure and N. N. Misra, *J. Eng. Process. Manage.*, 2020, **11**(2), DOI: **10.7251/jepm1902073u**.
45 T. Zhang, L. He, M. Zhang and H. Jiang, *Sci. Rep.*, 2024, **14**, 24366.
46 S. Jaddu, S. Sonkar, D. Seth, M. Dwivedi, R. C. Pradhan, G. Goksen, P. K. Sarangi and A. R. Jambrak, *Food Chem.:X*, 2024, **22**, DOI: **10.1016/j.fochx.2024.101266**.
47 L. Zare, N. Mollakhalili-Meybodi, H. Fallahzadeh and M. Arab, *LWT–Food Sci. Technol.*, 2022, **155**, DOI: **10.1016/j.lwt.2021.112898**.
48 S. Verdú, F. Vásquez, E. Ivorra, A. J. Sánchez, J. M. Barat and R. Grau, *J. Cereal. Sci.*, 2015, **65**, 67–73.
49 A. Gamal and A. M. F. Elbaz, *J. Food Technol. Res.*, 2024, **5**, 110–122.
50 R. Thirumdas, C. Sarangapani and U. S. Annapure, *Food Biophys.*, 2015, **10**, 1–11.
51 N. Mollakhalili-Meybodi, M. Yousefi, A. Nematollahi and N. Khorshidian, *Eur. Food Res. Technol.*, 2021, **247**, 1579–1594.
52 S. Rout, P. K. Panda, P. Dash, P. P. Srivastav and C.-T. Hsieh, *Int. J. Mol. Sci.*, 2025, **26**, 1564.

53 D. Das, A. Kuna, L. Kata, N. N. Misra, H. K. Sudini and A. Das, *Curr. Sci.*, 2025, **128**, 818–826.
54 R. Zhou, R. Zhou, J. Zhuang, Z. Zong, X. Zhang, D. Liu, K. Bazaka and K. Ostrikov, *PLoS One*, 2016, **11**, e0155584.
55 B. Li, L. Peng, Y. Cao, S. Liu, Y. Zhu, J. Dou, Z. Yang and C. Zhou, *Foods*, 2024, **13**, 1522.
56 M. Bayati, M. N. Lund, B. K. Tiwari and M. M. Poojary, *Compr. Rev. Food Sci. Food Saf.*, 2024, **23**(4), DOI: **10.1111/1541-4337.13376**.
57 Y. Wu, X. Feng, Y. Zhu, S. Li, Y. Hu, Y. Yao and N. Zhou, *Foods*, 2023, **12**, 3260.
58 C. Charu, S. Vignesh, D. Chidanand, R. Mahendran and N. Baskaran, *Food and Humanity*, 2024, **2**, 100238.
59 O. O. Olatunde, A. Hewage, T. Dissanayake, R. E. Aluko, A. C. Karaca, N. Shang and N. Bandara, *Compr. Rev. Food Sci. Food Saf.*, 2023, **22**, 2197–2234.
60 S. Basak and U. S. Annapure, *Future Foods*, 2022, **5**, 100119.
61 P. Pal, P. Kaur, N. Singh, A. Kaur, N. N. Misra, B. K. Tiwari, P. J. Cullen and A. S. Virdi, *Food Res. Int.*, 2016, **81**, 50–57.
62 M. Amiri, M. Arab and A. M. Mortazavian, *Sci. Rep.*, 2025, **15**(1), DOI: **10.1038/s41598-025-10281-x**.
63 Y. Bao, L. Reddivari and J. Y. Huang, *Innov. Food Sci. Emerg. Technol.*, 2020, **65**, 102445.
64 S. Sadhu, R. Thirumdas, R. R. Deshmukh and U. S. Annapure, *LWT–Food Sci. Technol.*, 2017, **78**, 97–104.
65 R. Coorey, A. Tjoe and V. Jayasena, *J. Food Sci.*, 2014, **79**(5), DOI: **10.1111/1750-3841.12444**.
66 X. Ge, H. Shen, C. Su, B. Zhang, Q. Zhang, H. Jiang and W. Li, *Food Chem.*, 2021, **349**, 129159.
67 A. M. G. Darwish, R. E. Khalifa and A. El, *Alexandria Sci. Exch. J.*, 2018, **39**, 450–459.
68 P. Carrión-Prieto, P. Martín-Ramos, S. Hernández-Navarro, I. Silva-Castro, M. Ramos-Silva and J. Martín-Gil, *Pharmacogn. J.*, 2017, **9**, 157–162.
69 M. Laçin and A. Başman, *Food Nutr. Sci.*, 2025, **13**(6), DOI: **10.1002/fsn3.70308**.
70 Y. P. Timilsena, R. Adhikari, C. J. Barrow and B. Adhikari, *Food Chem.*, 2016, **212**, 648–656.
71 A. M. Herrero, C. Ruiz-Capillas, T. Pintado, P. Carmona and F. Jimenez-Colmenero, *Food Chem.*, 2017, **221**, 1333–1339.
72 F. Sadeghi, A. Koocheki and F. Shahidi, *Food Hydrocoll.*, 2021, **120**, 106902.